Conf-920913--21

GA–A21053

REGIMES OF IMPROVED CONFINEMENT AND STABILITY IN DIII–D OBTAINED THROUGH CURRENT PROFILE MODIFICATIONS

by
L.L. LAO, J.R. FERRON, T.S. TAYLOR, V.S. CHAN
T.H. OSBORNE, K.H. BURRELL, M.S. CHU, J.C. DeBOO,
E.J. DOYLE, C.M. GREENFIELD, R.J. GROEBNER, G.L. JACKSON,
R. JAMES, E.A. LAZARUS, C. RETTIG, H. St JOHN,
E.J. STRAIT, S.J. THOMPSON, A.D. TURNBULL, D. WROBLEWSKI,
H. ZOHM, and THE DIII–D TEAM

SEPTEMBER 1992

GENERAL ATOMICS

DISCLAIMER

GA-A--21053

DE93 002674

REGIMES OF IMPROVED CONFINEMENT AND STABILITY IN DIII–D OBTAINED THROUGH CURRENT PROFILE MODIFICATIONS

by

L.L. LAO, J.R. FERRON, T.S. TAYLOR, V.S. CHAN
T.H. OSBORNE, K.H. BURRELL, M.S. CHU, J.C. DeBOO,
E.J. DOYLE,* C.M. GREENFIELD, R.J. GROEBNER, G.L. JACKSON,
R. JAMES,† E.A. LAZARUS,‡ C. RETTIG,* H. St JOHN,
E.J. STRAIT, S.J. THOMPSON, A.D. TURNBULL, D. WROBLEWSKI,†
H. ZOHM,[b] and THE DIII–D TEAM

This is a preprint of a combined paper to be presented at the Fourteenth International Conference on Plasma Physics and Controlled Nuclear Fusion Research, September 30 through October 7, 1992, Würzburg, Germany, and to be printed in the *Proceedings.*

Work supported by
U.S. Department of Energy
Contract Nos. DE-AC03-89ER51114, DE-AC05-OR21400,
and W-7405-ENG-48

* University of California at Los Angeles.
† Lawrence Livermore National Laboratory.
‡ Oak Ridge National Laboratory.
[b] Max Planck Institut für Plasmaphysik, Germany.

GENERAL ATOMICS PROJECT 3466
SEPTEMBER 1992

GENERAL ATOMICS

IAEA No. CN–56/A–7–19

REGIMES OF IMPROVED CONFINEMENT AND STABILITY IN DIII–D OBTAINED THROUGH CURRENT PROFILE MODIFICATIONS*

ABSTRACT

Several regimes of improved confinement and stability have been obtained in recent experiments in the DIII–D tokamak by dynamically varying the toroidal current density profile to transiently produce a poloidal magnetic field profile with more favorable confinement and stability properties. A very peaked current density profile with high plasma internal inductance, ℓ_i, is produced either by a rapid change in the plasma poloidal cross section or by a rapid change in the total plasma current. Values of thermal energy confinement times nearly 1.8 times the JET/DIII–D ELM–free H–mode thermal confinement scaling are obtained. The confinement enhancement factor over the ITER89–P L–mode confinement scaling, H, is as high as 3. Normalized toroidal beta, β_N, greater than 6 %-m-T/MA and values of the product $\beta_N H$ greater than 15 have also been obtained. Both the confinement and the maximum achievable β vary with ℓ_i and decrease as the current profile relaxes. For strongly shaped H–mode discharges, in addition to the current density profile peakedness, as measured by ℓ_i, other current profile parameters, such as its distribution near the edge region, may also affect the confinement enhancement.

1. INTRODUCTION AND OVERVIEW

The study of plasma stability and energy confinement as well as methods to improve them has been a very active area of tokamak research. These improvements may be measured by the normalized beta, $\beta_N \equiv \beta_T/(I/aB)$, and the confinement enhancement factor over the ITER89–P L–mode confinement scaling [1], $H \equiv \tau_E/\tau_{ITER89-P}$. Improved tokamak performance in both β_N and H concomitantly is desirable, which, together with an advance in the area of heat flux handling capability of the plasma facing components in the first wall, can potentially lead to a more compact and economically more attractive reactor.

In recent DIII–D tokamak experiments, several regimes of improved confinement and stability have been obtained by dynamically varying the toroidal current density profile to transiently produce a poloidal magnetic field profile with more favorable confinement and stability properties against instabilities and turbulence such as those driven by the pressure gradient. Confinement enhancement factors, H, ~3 and thermal energy confinement times normalized to the JET/DIII–D ELM–free H–mode thermal confinement value [2], $\tau_N \equiv \tau_{TH}/\tau_{JET/DIII-D}$, ~1.8 have been obtained, $\tau_{JET/DIII-D}$(s) $\equiv 0.106\ P_L^{-0.46}$ (MW) $I^{1.03}$ (MA) $R^{1.48}$(m). β_N greater than 6 %-m-T/MA and values of the

* Work sponsored by the U.S. Department of Energy under Contract Nos. DE-AC03-89ER51114, DE-AC05-84OR21400, and W-7405-ENG-48.

product $\beta_N H$ greater than 15 have also been obtained. The current profile is varied either by a rapid change in the plasma poloidal cross section or by a rapid change in the total plasma current to produce a very peaked current density profile with high plasma internal inductance, ℓ_i. Both the confinement and the maximum achievable β improve with increase in ℓ_i and decrease as the current profile relaxes.

In elongation ramp experiments, a very peaked toroidal current density profile is transiently produced by dynamically increasing the discharge elongation, κ, at a very fast rate, $\dot{\kappa} > 2/s$, after initiation of the auxiliary beam heating phase. Since the current diffusion time in the hot plasma center is long relative to that in the edge region, the current channel is trapped in the plasma core producing a very peaked current density profile. Both the input beam power, P_{NBI}, and the plasma current, I, are held fixed during the κ ramp. The κ ramp serves both to create a peaked current density profile as well as to induce an L–mode to H–mode transition. ELMing H–mode plasmas are obtained when the maximum κ exceeds 1.8. The energy confinement improves with ℓ_i and then decreases as the current profile relaxes and ELMing occurs.

In current ramp experiments, a peaked current density with small or negative edge current is transiently produced by rapidly decreasing I at a fast rate, $\dot{I}$, up to –4 MA/s. Experiments were performed in $\kappa \sim 1.2$ L–mode limiter plasmas, $\kappa \sim 1.7$ L–mode and H–mode limiter plasmas, as well as $\kappa \sim 2$ H–mode divertor plasmas [3]. The improvement in the energy confinement is found to correlate with the increase in ℓ_i, as is observed in current ramp experiments in L–mode plasmas in various other tokamaks [4–7], except in an experiment in H–mode divertor geometry. In a current ramp experiment in $\kappa \sim 2$ H–mode divertor plasmas, the plasma stored energy W is observed to follow I and decrease rapidly shortly after the current ramp phase begins, despite a large increase in ℓ_i.

Although both the κ ramp and the current ramp techniques produce a peaked current density profile with high ℓ_i, the details of the current density distribution in the edge region may be different depending on the details of the operations. The current ramp method obtains a peaked profile transiently by driving the loop voltage negative which tends to reduce the edge current density and, at a sufficiently fast ramp rate, can make it negative. In the κ ramp case, peaking of the current density profile is accomplished by adding cold plasma to the edge region at a fast rate so that most of the current is trapped in the core, which tends to give rise to a low but positive edge current density. The difference between the current ramp results in divertor H–mode plasmas and the κ ramp results suggest that for strongly shaped H–mode discharges, in addition to the current density profile peakedness, as measured by ℓ_i, other current profile parameters such as its distribution near the edge region may also play a role in the confinement enhancement.

The current ramp technique has also been used to produce discharges with high β_N as well as high H in $\kappa \sim 1.2$ L–mode plasmas. The maximum obtainable β_N is observed to increase approximately linearly with ℓ_i, as is observed in confinement experiments. The result is consistent with both analytical and numerical predictions of the scaling of the β limit with ℓ_i based on the ideal ballooning mode theory [8]. Only very limited attempts have been made to study high $\beta_N H$ plasmas using the κ ramp technique. The $\beta_N H$ values obtained in these current profile modification experiments are among the highest that have been achieved in DIII–D.

The results of the κ ramp experiments are summarized in the next section. This is followed by a discussion of the current ramp experiments in Section 3. In Section 4, a summary of the high $\beta_N H$ discharges obtained using these two techniques is given. Finally, a conclusion is given in Section 5.

2. ELONGATION RAMP EXPERIMENTS

The κ ramp experiments are motivated by the confinement results from current ramp experiments in L–mode limiter plasmas from various other tokamaks [4–6], as well as the beta and the confinement results from current ramp experiments in DIII–D [3] which are described in the next section. The experiments are designed to further test the effects of toroidal current density profile on energy confinement by making use of the unique shaping capability of DIII–D to vary the current profile by a rapid change in the plasma poloidal cross section. Unlike the current ramp method, which simultaneously varies both the shape of the current profile and the total plasma current, I, the κ ramp technique is capable of varying only the shape of the current density profile while keeping I constant. Thus, the experiments can yield additional insight into the effects of current density profile on energy confinement.

In Fig. 1, a time history of an H–mode discharge obtained using the κ ramp technique is given. Also shown are the plasma poloidal cross sections at various times. κ is programmed to increase from 1.3 to greater than 1.8 in 200 ms with I and P_{NBI} held fixed at 1 MA and 5.7 MW, respectively. As κ is increased, W and τ_N first decrease slightly and then increase with ℓ_i. Around 2120 ms, when $\ell_i \sim 1.8$ and $\kappa \sim 1.8$, the plasma transits into the H–mode phase and τ_N increases rapidly from about 0.9 to nearly 1.8 and then slowly decays back to 1.1 near the end of the beam heating phase at 4000 ms. After the L–H transition, ℓ_i continues to increase from 1.8 to nearly 1.9 and then slowly decays to about 1.2 as the current profile relaxes. The surface voltage, V_S, increases rapidly from 1 to nearly 3 V during the early phase of the κ ramp, and then decreases to $\sim$–0.3 V near the end of the ramp. As the current profile relaxes, V_S slowly rises back to $\sim$0.1 V at 4000 ms. Also shown in Fig. 1 is a reference $\kappa \sim 2.1$ H–mode discharge with $\ell_i \sim 1$ and $\tau_N \sim 0.9$. Note that unlike the current ramp experiments in L–mode plasmas, where W and τ_E are observed to decay slowly and only τ_N is observed to increase, here, in addition to τ_N, both W and τ_E are found to actually improve following the change in the current profile shape.

The τ_N variation during the slow current relaxation phase correlates well with the change in ℓ_i. After the H–mode transition, the discharge stays ELM–free for about 240 ms and then starts ELMing. Despite the presence of ELMs, the energy confinement remains higher than values expected using the JET/DIII–D ELM–free H–mode scaling. Although the discharge has a very peaked current density profile and reaches $\kappa \sim 2.1$ at $\ell_i \sim 1.9$, stability analysis of MHD equilibria reconstructed using kinetic profile and magnetic data (described below) shows it is stable to the ideal axisymmetric mode with a conducting wall at the vacuum vessel surrounding the plasma and unstable if the wall is more than 25% away.

The improvement in confinement is observed in both the density and the temperature profiles. This is illustrated in Fig. 2, where the density and the temperature profiles at 2500 ms when $\ell_i \sim 1.7$ and $\tau_N \sim 1.6$ are compared against

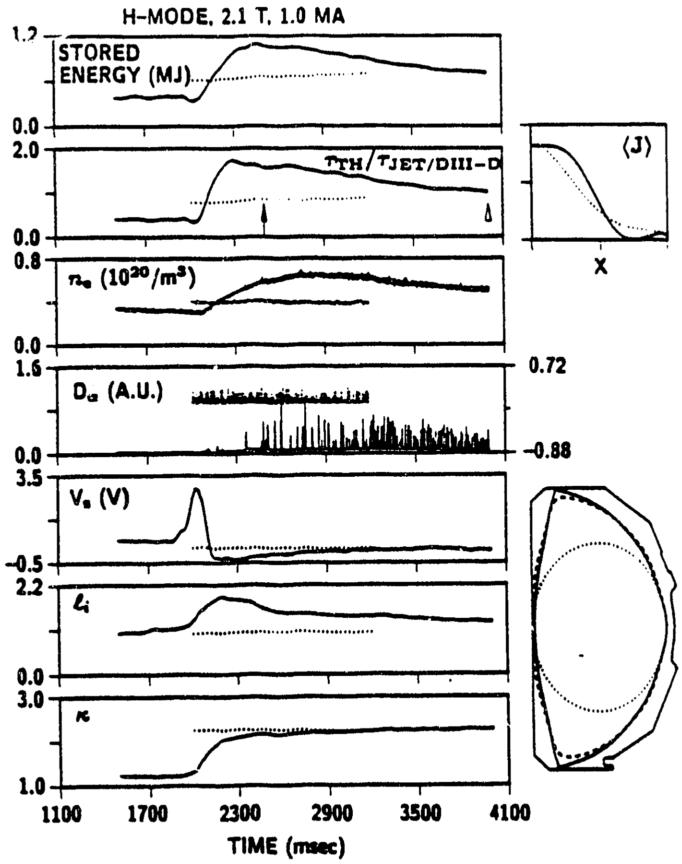

Fig. 1. Time evolution of the plasma stored energy, the normalized thermal energy confinement time, the line-averaged electron density, divertor D_α radiation, the surface voltage, the internal inductance, and the elongation for a κ ramp discharge with $P_{NBI} = 5.7$ MW (solid traces) and a constant κ H-mode reference discharge with $P_{NBI} = 6.2$ MW (dotted traces). For visibility, the D_α trace for the reference discharge is shown with an offset. Also shown are the plasma boundary shapes at 1950 ms (dotted curve), 2150 ms (dashed curve), 2350 ms (solid curve) and $\langle J \rangle$ at 2500 ms (solid curve) and 4000 ms (dotted curve) for the κ ramp discharge. The two times 2500 and 4000 ms are indicated by arrows.

those at 4000 ms when $\ell_i \sim 1.2$ and $\tau_N \sim 1.1$. Transport analysis using the measured profiles shows that the effective single fluid thermal diffusivity, χ_{eff}, is significantly reduced over most of the plasma cross section at the high ℓ_i time, although the uncertainty is large.

The flux surface average current density profiles, $\langle J \rangle$, at these two times reconstructed from equilibrium analysis [9] using the measured kinetic profiles, the external magnetic measurements, and a single channel Motional Stark Effect (MSE) measurement [10] are given in Fig. 1. Reconstruction results using the newly installed eight-channel MSE current profile diagnostic [11] and magnetic data for a similar discharge show current density profiles with similar shapes.

The reconstructed current density profiles show a small but positive current density near the edge region as well as an improvement of the parameter,

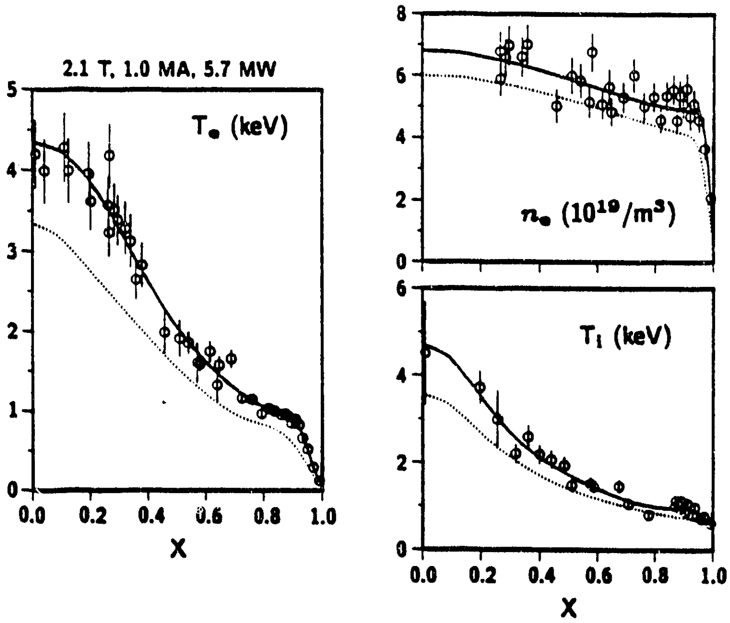

Fig. 2. Comparison of electron temperature profiles from Thomson scattering and horizontal ECE, electron density profiles from Thomson scattering and interferometry, and ion temperature profiles from CER at 2500 ms (open circles and solid curves) and at 4000 ms (dotted curves) for a κ ramp discharge.

$\mu \equiv S/q^2$, in the plasma outer region $x > 0.4$ at the high ℓ_i time. The small positive edge current density may play a role in the confinement enhancement and is discussed in the next section. The parameter μ characterizes the stabilization effects against pressure driven instabilities and turbulence due to the improvement in the magnetic shear, S, and the reduction in the connection length between the good and the bad curvature regions. Here, $0 \leq x \leq 1$ is a normalized equivalent minor radius. The reduction of χ_{eff} in the region $x > 0.4$ is consistent with the increase of μ in this region. However, in the region $x < 0.4$, χ_{eff} still shows a reduction despite a smaller μ at the high ℓ_i time. This suggests a weak dependence of χ_{eff} on S in this region.

The confinement data obtained from several κ ramp discharges during the slow current relaxation phase with I = 1.0–1.5 MA and P_{NBI} = 4–12 MW are summarized in Fig. 3. τ_N is observed to vary approximately linearly with ℓ_i. The results are similar to those obtained in current ramp experiments in L-mode plasmas in various other tokamaks [4–7] and in L-mode and H-mode limiter plasmas in DIII–D [3] as described in the next section.

3. CURRENT RAMP EXPERIMENTS

Improved confinement has been observed with the use of current ramping in limiter H-mode discharges. A time history of a $\kappa \sim 1.7$ limiter H-mode discharge obtained using the current ramp technique is given in Fig. 4. Also shown are the flux surfaces at 3300 ms near the time of peaked stored energy when $\ell_i \sim 2.0$

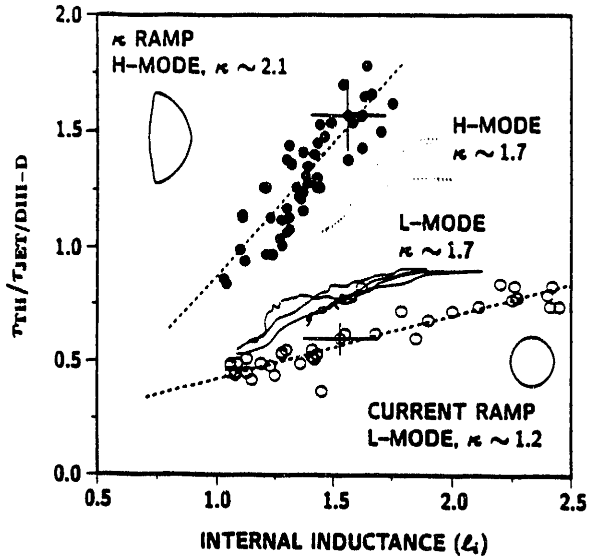

Fig. 3. Variation of the normalized thermal energy confinement time with ℓ_i for data obtained from κ ramp experiments (solid circles) and current ramp experiments in $\kappa \sim 1.2$ limiter L–mode plasmas (open circles), $\kappa \sim 1.7$ limiter L–mode plasmas (solid curves), and $\kappa \sim 1.7$ limiter H–mode plasmas (dotted curves), $\tau_{JET/DIII-D}$ (s) $\equiv 0.106\ P_L^{-0.46}$ (MW) $I^{1.03}$ (MA) $R^{1.48}$ (m).

and $\tau_N \sim 1.6$ and at 4200 ms near the end of the H–mode phase when $\ell_i \sim 1.4$ and $\tau_N \sim 1.1$. $\langle J \rangle$ at these two times, reconstructed from the external magnetics and the eight-channel MSE data, are also given in Fig. 4. I is decreased from 2 to 1 MA in ~700 ms with $P_{NBI} \sim 4.2$ MW. The discharge shape evolves slowly from an inside limiter to become marginally diverted in the top after transition into the H–mode phase due to the changes in the current profile caused by the current ramp. V_S decreases from 0.6 V before the current ramp phase to ~ –1 V near the end of the current ramp phase. As shown in Fig. 4, at the high ℓ_i time $\langle J \rangle$ near the edge is negative.

The energy confinement is observed to vary with ℓ_i. The plasma transits into the H–mode phase during the current ramp near 3030 ms with a relatively short ELM–free period. ℓ_i increases from 1.1 in the L–mode phase before the current ramp to greater than 2 after transition into the H–mode phase and then decreases to ~1.4 near the end of the H–mode phase as the current profile relaxes. Concurrently, τ_N increases from about 0.5 to nearly 1.6 and then decreases to around 1. As the current profile broadens, the discharge transits back into the L–mode phase with $\tau_N \sim 0.5$ after 4300 ms, which is often observed in these discharges. Similar improvement of τ_N with ℓ_i is also observed in current ramp experiments in $\kappa \sim 1.2$ and ~1.7 L–mode limiter plasmas. The data from these current ramp experiments are summarized in Fig. 3. In addition to the ℓ_i dependence, the data may also indicate a possible dependence of τ_{TH} on κ.

In contrast, no improvement of confinement with ℓ_i is found in a current ramp experiment in $\kappa \sim 2$ ELMing divertor H–mode plasmas [3]. I is ramped down during the ELMing phase of an H–mode discharge, rather than during the L–mode phase as in the limiter H–mode case, and at a faster rate, from 2

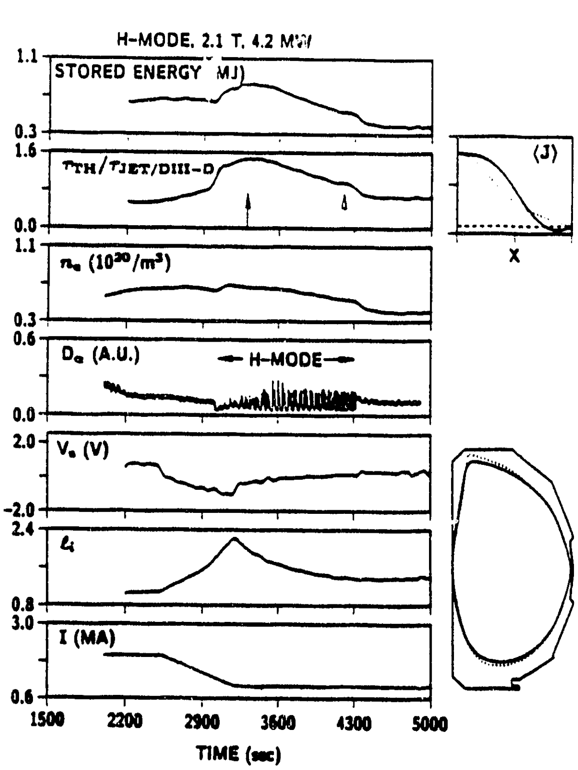

Fig. 4. Time evolution of the plasma stored energy, the normalized thermal energy confinement time, the line-averaged electron density, inside wall D_α radiation, the surface voltage, the internal inductance, and the total plasma current for a current ramp discharge, P_{NBI} = 4.2 MW. Also shown are the plasma boundary shapes and $\langle J \rangle$ at 3300 ms (solid curves) and at 4200 ms (dotted curves). The two times 3300 and 4200 ms are indicated by arrows.

to 1 MA in about 300 ms, with $P_{NBI} \sim 7.3$ MW. W is observed to follow I and decrease during the current ramp phase from ~1.5 MJ to ~1.0 MJ despite a large increase in ℓ_i from nearly 1.1 to greater than 2. A drop in electron density of as much as 60%, primarily in the outer plasma region, is observed. During the current ramp, κ varies from ~2 to ~1.7 due to the effects of the large increase of ℓ_i on the discharge shape control system. Although the interpretation of this experiment is complicated by this variation in κ, the difference between the results from this experiment and those from κ ramp and other current ramp experiments suggest that in addition to the peakedness of the current density profile, as measured by ℓ_i, for strongly shaped H-mode plasmas other current profile parameters, such as their detail distribution near the edge region, may also play a role in the confinement enhancement by affecting the steep edge pressure gradients often observed in H-mode discharges. In DIII-D H-mode discharges with low edge current density, the edge pressure gradients are limited by the first ideal ballooning mode stability [12]. In strongly shaped divertor plasmas, the ballooning stability boundary is sensitive to the details of the edge current density distribution.

4. HIGH $\beta_N H$ DISCHARGES

The current ramp technique has also been used to study the effects of current profile on β limits. The results of a β experiment in $\kappa \sim 1.2$ L–mode near circular plasmas are summarized in Fig. 5. $\beta_N > 6$ %-m-T/MA and values of the product $\beta_N H > 15$ have been obtained by rapidly ramping down the plasma current at a fast rate, $\dot{I} < -2$ MA/s, to produce a peaked current density profile with ℓ_i as high as 2.

The maximum obtainable β_N is observed to increase approximately linearly with ℓ_i, as is observed in confinement experiments. This result is consistent with both analytical and numerical theoretical predictions of the scaling of the β limit with ℓ_i based on the ideal ballooning stability theory [8]. Also shown in Fig. 5 are the ideal ballooning β limits computed numerically using MHD equilibria corresponding to these discharges reconstructed from external magnetic data. Detailed ideal stability analysis for a discharge near its peaked $\beta_N \sim 6$%-m-T/MA time using equilibrium reconstructed from measured kinetic profile, magnetic, and a single channel MSE data with a conducting wall at the vacuum vessel shows that it is unstable to a 1/1 internal mode if the axial safety factor, $q(0)$, is less than 1 and stable to the $n = 1$ kink mode if $q(0)$ is greater than 1. The equilibrium is marginally stable to the ideal ballooning mode. The $n = 1$ calculation results are consistent with the fishbone oscillations often observed in these discharges.

Only very limited attempts have been made to study the effects of current density profile on β limits using the κ ramp technique. In a κ ramp experiment at a magnetic field, B, of 0.86 T, β_N greater than 5 and values of the product $\beta_N H$ close to 13 have been obtained in a divertor H–mode discharge.

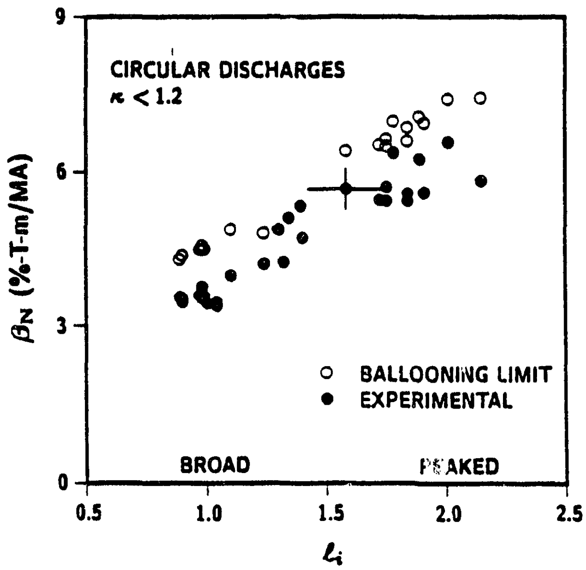

Fig. 5. Variation of the normalized beta, β_N, with ℓ_i from a current ramp experiment in limiter L–mode plasmas. Measured values and the corresponding calculated ballooning mode limits are shown.

The $\beta_N H$ values obtained in these current profile modification experiments are among the highest that have been achieved in DIII–D, although they are modest in terms of the absolute values in β and τ_E. These are summarized in Fig. 6 along with the rest of the data in the DIII–D beam heated deuterium plasma database. The results suggest that with proper current profile control high performance tokamak operation is possible. Also shown in Fig. 6 is a theoretical limit for $\beta_N H$ [13] derived from the β scaling expression, $\beta \le C_\beta I/aB$,

$$\beta_N H \le \frac{C_{\beta H}\, \epsilon^{0.7}\, \sqrt{d}\, B^{0.8}\,(\mathrm{T})\ I^{0.15}\,(\mathrm{MA})}{a\,(\mathrm{m})\,\sqrt{P_V\,(\mathrm{MW/m^3})}\ n^{0.1}\ (10^{20}/\mathrm{m^3})}\ , \tag{1}$$

where $P_V = P_T/V$, $d = V/(2\pi^2 R a^2 \kappa)$, V is the plasma volume, P_T is the total heating power, and ϵ is the inverse aspect ratio. Here, $C_{\beta H} \approx 8\ell_i^2$ for $C_\beta = 4.5\,\ell_i$. Equation (1) can be viewed as a form of the β limit rewritten to emphasize the confinement as well as the β aspects of this limit. These are discussed in detail in Ref. [13]. The observation that there are quite a number of data points from these profile modification experiments as well as many from VH–mode experiments [14] with enhanced confinement and high $\beta_N H$ values lying close to the β limit suggests that operating close to the β limit may not necessarily lead to poor plasma performance.

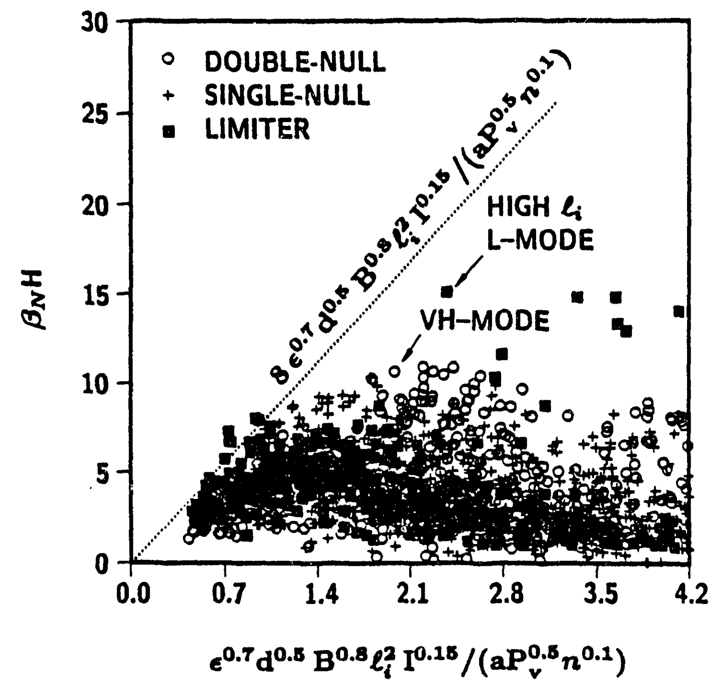

Fig. 6. Comparison of $\beta_N H$ values from current profile modification experiments and those from the DIII–D beam heated deuterium database.

5. CONCLUSION

The results from these experiments indicate that high energy confinement and high β are obtainable with a peaked current density profile (high ℓ_i), sufficient degree of shaping, and perhaps some requirement for edge current density. With detailed current and heating profile control in shaped tokamak discharges, steady state and high performance tokamak operation may be possible.

REFERENCES

[1] YUSHMANOV, P.N., TAKIZUKA, T., RIEDEL, K.S., *et al.*, Nucl. Fusion **30** (1990) 1999.

[2] SCHISSEL, D.P., DeBOO, J.C., BURRELL, K.H., *et al.*, Nucl. Fusion **31** (1991) 73.

[3] FERRON, J.R., LAO, L.L., TAYLOR, T.S., in Controlled Fusion and Plasma Physics (Proc. 19th European Conf., Innsbruck, 1992), Vol. 16C, Part I, EPS (1992) 55.

[4] ZARNSTORFF, M.C., BARNES, C.W., EFTHIMION, P.C., *et al.*, in Plasma Physics and Controlled Nuclear Fusion Research (Proc. 13th International Conf., Washington, DC, 1990), IAEA, Vienna, 1991, Vol. I, p. 109.

[5] O'ROURKE, J., BALET, B., CHALLIS, C., *et al.*, in Controlled Fusion and Plasma Physics (Proc. 18th European Conf., Berlin, 1991), Vol. 15C, Part I, European Physical Society (1991) p. 37.

[6] MURMANN, H., ZOHM, H., *et al.*, in Controlled Fusion and Plasma Physics (Proc. 17th European Conf., Amsterdam, 1990), Vol. 14B, Part I, European Physical Society (1990) p. 54.

[7] HOANG, G.T., BIZARRO, J.P., *et al.*, in Controlled Fusion and Plasma Physics (Proc. 19th European Conf., Innsbruck, 1992), Vol. 16C, Part I, European Physical Society (1992) p. 27.

[8] LAO, L.L., TAYLOR, T.S., CHU, M.S., *et al.*, Phys. Fluids B **4** (1992) 232.

[9] LAO, L.L., FERRON, J.R., GROEBNER, R.J., *et al.*, Nucl. Fusion **30** (1990) 1035.

[10] WROBLEWSKI, D., BURRELL, K.H., LAO, L.L., *et al.*, Rev. Sci. Instrum. **61** (1990) 3552.

[11] WROBLEWSKI, D., LAO, L.L., General Atomics Report GA–A20881, to be published in Rev. Sci. Instrum. (1992).

[12] GOHIL, P., MAHDAVI, M.A., LAO, L.L., *et al.*, Phys. Rev. Lett. **61** (1988) 1603.

[13] CHAN, V.S., LAO, L.L., TAYLOR, T.S., General Atomics Report GA–A20973 (1992), to be submitted to Nucl. Fusion.

[14] JACKSON, G.L., WINTER, J., TAYLOR, T.S., *et al.*, Phys. Rev. Lett. **67** (1991) 3098.

DATE
FILMED
01/20/93